New Approach-based MPP Tracking Design for Standalone PV Energy Conversion Systems

Sy Ngo[1, *], Chian-Song Chiu[2], Thanh-Dong Ngo[1], Cao-Tri Nguyen[1]
[1]*Institute of Engineering and Technology, Thu Dau Mot University, Binh Duong, Vietnam*
[2]*Department of Electrical Engineering, Chung Yuan Christian University, Taoyuan City, Taiwan 32023, R.O.C*
[*]*syn@tdmu.edu.vn, cschiu@cycu.edu.tw, dongnt@tdmu.edu.vn, trinc@tdmu.edu.vn*

***Abstract*—In searching for a maximum power point (MPP) using a DC boost converter for photovoltaic (PV) energy conversion systems, we realised that the fast and accurate way to find the suitable duty ratio (d_r) value is the core problem to enhance the energy conversion efficiency of the PV system. Under uniform irradiation, the panels will generate the same values, so they have only one peak on the P-V curve; conventional MPP tracking methods easily obtain this MPP. However, under partial shading conditions, many peaks are created, traditional MPP tracking methods can fall into the local MPP, and this issue will cause energy loss and reduce PV energy conversion efficiency. To avoid this disadvantage, this paper proposes a hybrid method (HM) by combining the improved chicken swarm optimisation (CSO) method and the incremental conductance (InC) algorithm for a DC standalone PV energy conversion system. In this hybrid method, the improved CSO modified approach is used to search the global region, and the InC algorithm is responsible for capturing the top of this global region. MATLAB simulation and experimental results were performed to demonstrate that the proposed method has achieved the global MPP under uniform solar irradiance and partial shadow effects.**

***Index Terms*—Partial shadow effects; Photovoltaic (PV); Boost converter; Maximum power point (MPP); Direct current (DC); Chicken swarm optimisation (CSO); Duty ratio.**

I. INTRODUCTION

Wind energy and photovoltaic (PV) energy are the two most popular clean energy sources used in the renewable energy system. They have been exploited strongly in recent years. The benefits of PV energy are not polluting, universal, and inexhaustible energy source. It has become one of the most widely used alternative energy sources. Many authors have researched the MPP tracking control of the PV system utilising the hill climbing (HC) [1], perturbation and observation (P&O) [2], incremental conductance (InC) [3] algorithms, etc. to increase the efficiency of PV energy conversion. In addition, the PV energy source also has the disadvantage that the radiation intensity is unstable and heterogeneous due to the conditions of clouds, trees, environmental factors, the direction of the sun. These traditional methods will easily be fallen into the local MPP, this situation will cause energy loss and reduce the PV power conversion efficiency. Researchers have tried to address these impacts through various enhanced adjustments to increase the efficiency of the energy conversion of the PV power system [4]. Unfortunately, finding a perfect solution is still difficult. They will be lagging during dynamic processing if these upgraded solutions perform well in a steady state, and vice versa. In addition, some solutions have performed relatively well, but they are quite complex in computational and design constraints when implemented on low-cost processors.

Due to partial shadow effects, the P-V curve of the PV panels will be transferred from the single peak to many peaks. In these peaks, there is one global MPP and several local MPPs. In this situation, the optimal MPP tracking solution is required to effectively track the global MPP and avoid the local MPPs. For that reason, many methods have been proposed such as the artificial neural network (ANN) technique [5], the particle swarm optimisation (PSO) [6], the grey wolf optimisation [7], and the butterfly optimisation algorithm [8]. The variety of MPP tracking methods for searching the maximum power point under partial shadow effects has been developed and can be classified into two styles: soft computing-based MPP tracking methods [9] and hardware-based MPP tracking methods [10]. In this case, soft computing-based MPP tracking methods are more strongly developed. They are referred to as heuristic algorithms [11], improved heuristic algorithms [12], and hybrid algorithms. The hybrid approach combines traditional and heuristic techniques, such as an enhanced P&O algorithm merged with an artificial bee colony [13], an incremental conductance-based particle swarm optimisation algorithm [14], or a combination of two heuristic techniques [15]. The main goals of these methods are to quickly search for the MPP in the global region, simple calculation, and the output power of the PV system has low amplitude oscillation [16].

Based on the databases of the above researches, the authors of this paper has used the proposed hybrid method and a DC boost converter to search the MPP of the PV panels and transfer this search power into the load [17]. In this research, a new technique is proposed to search for the global MPP and improve the energy conversion efficiency of the PV array. The idea is derived from the results of the

Manuscript received 13 September, 2022; accepted 25 January, 2023.

aforementioned hybrid methods. The proposed idea of this combining method is to use an improved chicken swarm optimisation (CSO) method to find quickly in the global region and move to the InC algorithm to achieve the MPP in this global region [18]. However, since the movement of frogs is random throughout the search area, it takes a long time to find the convergence position. The highlights of this improved CSO (ICSO) method are the selection, organisation, and simplification of the original chicken population. In addition, the new way to update positions based on the behaviour of chicks is also an advantage of the proposed solution. The arrangement and division of search areas are also a suitable solution for searching for the global region that has been adopted [19].

The details of the hybrid method will be presented in Section III. The remainder of this paper is structured as described in the following. The introduction of the PV energy system is in Section II. The PV array model, the partial shading scenarios, and the use of a DC/DC boost converter for MPP tracking are included. The proposed hybrid method, which combines the InC algorithm and the improved CSO method, is described in Section III for the MPP tracking control of the PV energy system. The results of the MPP tracking simulation are shown in Section IV. Finally, in the concluding section, the findings are offered.

TABLE I. SYMBOLS AND DESCRIPTION FOR PV CELL.

Symbol	Description	Symbol	Description
N_p	Number of parallel panels	N_s	Number of serial panels
k_o	$k_o = A_s / kTB_s$	I_{ph}	Photocurrent
I_{sat}	Reverse saturation current	I_{sc}	Short-circuit current
T	Operating temperature	T_{ref}	Reference temperature
E_{gp}	$E_{gp} = 1.11ev$	λ	Irradiance intensity
A_s	Electronic charge $(1.6\times10^{-19}c)$	k	Boltzmann's constant $1.38\times10^{-23}(J/K)$
B_s	Ideal P-N junction factor	K_{tc}	Short-circuit current temperature coefficient
i_{pv}	Current of a PV cell	v_{pv}	Series resistance
R_s	Voltage of a PV cell	R_p	Shunt resistance

II. INTRODUCTION OF A PV ENERGY SYSTEM

A. Model of the PV Array

PV cell is the smallest part of the PV panel. Therefore, to achieve a higher voltage and power, the PV cell strings were connected in series and parallel to obtain the PV array $(N_s \times N_p)$ as shown in [19]. The output voltage V_{pv} and output current I_{pv}, and the characteristics of the PV array can be obtained:

$$I_{pv} = N_p[I_{ph} - I_{sat}(e^{(k_o V_{pv}/N_s)} - 1)], \quad (1)$$

$$P_{pv} = I_{pv}V_{pv} = V_{pv}N_p[I_{ph} - I_{sat}(e^{(k_o V_{pv}/N_s)} - 1)], \quad (2)$$

where I_{sat} is a reverse saturation current, $k_o = A_s / (kTB_s)$, A_s is the amount of charge of a single electron $(1.6\times10^{-19}c)$, T is the panel operating temperature (K), K is the Boltzmann constant $(1.38\times10^{-23}J/{}^oK)$, B_s is the ideal P-N junction characteristic factor of the PV cell, V_{pv} is the output voltage of the PV array, I_{pv} is the output current of the PV array, and P_{pv} is the output power of the PV array. The relationship between the current source I_{ph} generated by a single PV cell and the solar irradiance is

$$I_{ph} = [I_{sc} + (T - T_r)K_{tc}]\lambda / 100, \quad (3)$$

where I_{sc} is the short-circuit current at the reference temperature $T_r(K)$ and the solar irradiance condition $100\,mW/cm^2$, K_{tc} is the short-circuit current temperature coefficient $(mA/{}^oC)$ of the PV panel, and λ is the solar irradiance (mW/cm^2). Through (1) and (2), the current, voltage, and power curves of the PV array can be obtained for different atmospheric temperatures and solar irradiance conditions. When the temperature is fixed, the output power of the solar panel increases when the solar irradiance increases. Otherwise, when the solar irradiance is fixed, the output power decreases as the temperature increases. Therefore, a power controller is required to remove the effect due to varying temperature and solar irradiance to extract more electrical power from the solar energy system. In addition, when the PV system is operated under partial shading conditions, how to control this solar energy system operating at the global MPP to improve the energy conversion efficiency, is an important topic that needs to be investigated.

B. Partial Shading Conditions

In a practical application, a single PV panel cannot supply enough power and voltage due to its limited power capacity and voltage. PV panels are linked in series to enhance output voltage. PV panels can also be joined in series and parallel for greater power. To safeguard the PV system, each PV panel is parallel to a diode. Figure 1 shows how to connect the M-series PV panels. Each PV panel produces the same amount of current when the solar irradiation is equal for all of them. The output current and output voltage of the shaded PV panels will drop if one PV panel is covered by the environment (trees, clouds, etc.). In the worst-case situation, the parallel diode with the shaded PV panel will activate when the output current is zero. This will cause the diode to bypass the shaded PV panel, preventing the low output current from being restricted by the low solar irradiation of the shaded PV panel. In other words, the voltage of this shaded PV panel is zero when the parallel diode is turned on. For example, the PVM panel is shaded, and the parallel diode D_M of this shaded PV panel is turned on. The path of current in the PV panels is shown in Fig. 1. The voltage value of this shaded board will not be included in the overall output voltage of the PV array. Equation (1) allows the following expression to represent the output

voltage of the PV panel

$$v_{pv(k)} = \frac{N_s}{k_o}\ln\left(\frac{N_p I_{ph(k)} + N_p I_{sat} - i_{pv(k)}}{N_p I_{sat}}\right), \quad k = 1,2,...,M, \quad (4)$$

where $I_{ph(k)}$ depends on the solar irradiance and $v_{pv(k)}$ and $i_{pv(k)}$ are the output voltage and current of the k^{th} PV panels. In addition, to understand more about partial shading conditions, the solar irradiances are used with different radiation intensities and fixed ambient temperature 25 ^oC as illustrated in Fig. 2.

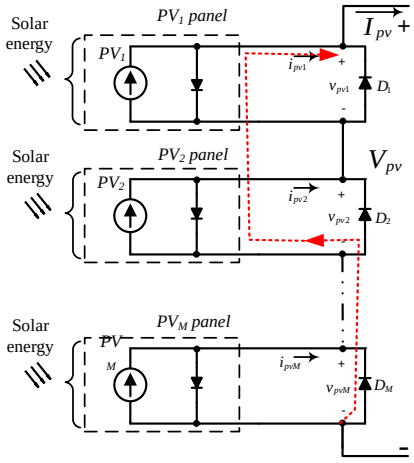

Fig. 1. Equivalent model of a PV string.

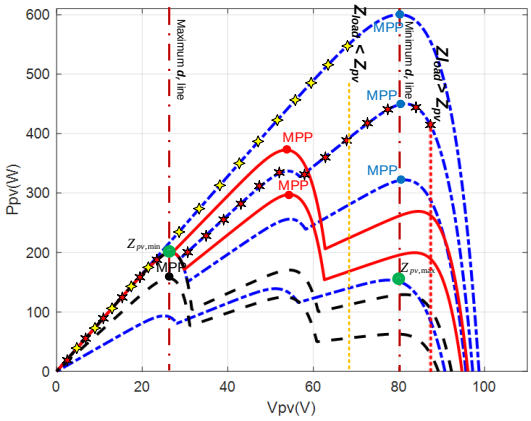

Fig. 2. P-V curves of the different cases of solar irradiance with M = 3 (panels).

With three panels connected in series, when the PV system is affected by partial shadows, three MPPs are created, one MPP of the global region and two MPPs in the local region. If M panels are irradiated with different solar intensities. They will be created M peaks with one global MPP and $(M-1)$ local peaks. The global MPP can be anywhere on the P-V curve (Fig. 2). If the global MPP is located on the "Minimum line", its PV impedance value is $Z_{pv,\min}$. Otherwise, if the global MPP is located on the "Maximum line", its PV impedance value is $Z_{pv,\max}$. If the global MPP falls within these two lines (red P-V curves), it will have a PV impedance value of $Z_{pv,GMPP}$, with $Z_{pv,\min} \le Z_{pv,GMPP} \le Z_{pv,\max}$.

C. *Usage of DC Boost Converter in MPP Tracking*

The basic architecture of the boost converter is illustrated in Fig. 3. The main task of this system is used in MPP tracking purposes for which output voltage boosting is required. This system is also used to provide impedance matching between PV panels and load with MPP tracking methods. The voltage and current of the PV panels are employed as the input parameters for the proposed MPP tracking system, and the output parameter is the duty ratio (d_r) of MPP tracking. The duty ratio (d_r) is determined by the mathematical function referred to as $Z_{pv} = f(d_r, Z_{Load})$. In this function, d_r is the pulse width modulation of the drive signal of the power switch in the DC boost converter, Z_{Load} is the impedance seen from the output side of the boost converter, Z_{pv} is the ratio of squared voltage and power of the PV panels at MPP, and this value depends on the solar irradiance intensity (Fig. 2). Assuming that the boost converter is 100 % efficient, to perform MPP tracking analysis of the boost converter, the mathematical function above can be written as follows

$$Z_{Load} = \frac{Z_{pv}}{(1-d_r)^2}. \quad (5)$$

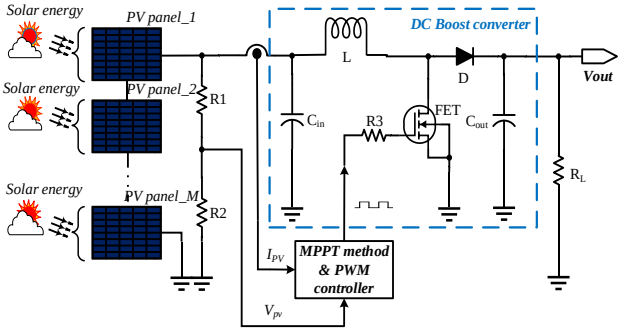

Fig. 3. Basic boost converter and control circuit for PV panels.

According to (5), Z_{Load} must be bigger than Z_{pv}. Therefore, the MPP tracking capability of the boost converter is limited ($D_{\min} \le d_r \le D_{\max}$). For example, in Fig. 2, the four-pointed yellow stars indicate the operating range of the PV panels for irradiance conditions and certain load. Since $Z_{Load} < Z_{pv}$ (dashed yellow line), the maximum available power cannot be obtained. Otherwise, if $Z_{Load} > Z_{pv}$ (dashed red line), the operation range will increase, and the maximum available power is realised efficiently, as shown on the six-pointed red stars in Fig. 2. Therefore, to select a certain load value, the value of the source impedance (Z_{pv}) should be predicted. This value is determined as in (6)

$$Z_{pv} = \frac{V_{pv,MPP}^2}{P_{pv,MPP}}. \quad (6)$$

The minimum and maximum values of the source impedance are calculated as in (7) and are seen in Fig. 2 with big green circles

$$Z_{pv,\min}=\frac{V_{pv,\max}^2}{P_{pv,\max}};Z_{pv,\max}=\frac{M\times V_{pv,\max}^2}{P_{MPP}}, \quad (7)$$

where M is the number of panels, $V_{pv,\max}$ and $P_{pv,\max}$ are the maximum value of the voltage and power of each panel, and P_{MPP} is the power value at the MPP.

III. Proposed Method Tracking Control

A. Improved CSO Method

Under a uniform radiance condition, the panels generate only one peak on the P-V curve, and conventional MPP tracking methods are easily obtained for this MPP. In other words, only one output impedance of the panels has the maximum power value. When PV panels are shaded by the environment, multiple MPPs are created. The energy conversion efficiency of the PV array will decrease if the conventional MPP tracking method is utilised, as it is simple to fall into the local MPP. Therefore, this paper proposes a combination, which is a hybrid method of the improved CSO and the various step size InC algorithm. The improved CSO is used to search the global maximum power region, which can avoid falling into the local regions. When the largest power value in the whole region is found, it will switch to the proposed InC algorithm to achieve the global MPP.

The global region search optimisation problem is solved using the chicken swarm optimisation (CSO) technique. The CSO, which was first introduced in [20], is regarded as one of the most modern heuristic optimisation methods. The hierarchical structure of the chicken swarm and its behaviours are the basis for this algorithm. To find food, the chicken swarm is split into several smaller groups, each of which consists of a rooster and a large number of hens and chicks. To find a global power region, this proposed CSO algorithm will be difficult to calculate, time-consuming, and complicated in an organisation.

In this paper, we proposed a new approach to the CSO method by reorganising the CSO method. In this improved CSO method, the chicken swarm consists of N chicks and only one mother hen. In the initial phase, N chicks are divided into N areas with increasing values from $D_{\min}$ to $D_{\max}$. Each chick will move randomly to find food within its area [19]. In this way, the global area is found quickly compared to the solution of using random chicken swarms without arrangement. Each chick will move randomly within its area as follows

$$d_{r,j}(k)=randi\left[(C_{\min}+(j-1)\Delta C_{step})\ \ (C_{\min}+j)\Delta C_{step}\right]/1000, \quad (8)$$

where $C_{\min}=1000D_{\min}$, $\Delta C_{step}=1000(D_{\max}-D_{\min})/N$, N is the number of chicks in the chicken swarm, and $D_{\min}$, $D_{\max}$ are the minimum, maximum limits of the duty ratio (d_r).

Each value of the duty ratio (d_r) will be used to control the power switch of the boost converter, and with this each value, the system will obtain a corresponding fitness value. Among these N values of the duty ratio (d_r), there will be one best fitness value called $d_{r,best}$ corresponding to the mother hen. The organisation of the ICSO method is shown in Fig. 4(a). The organisation, arrangement, and area division modelled from (8) are shown in Fig. 5(a).

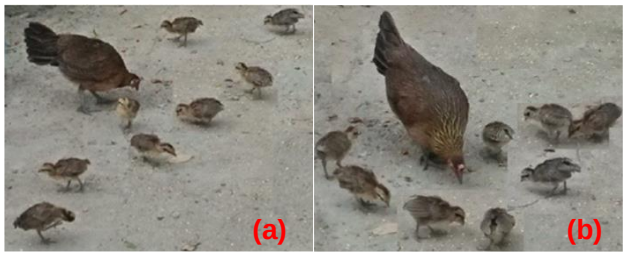

Fig. 4. The organisational model of the chicken flock.

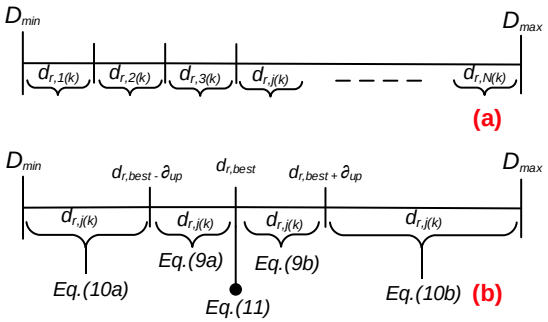

Fig. 5. The arrangement and division of the area of the chicks.

After determining the location of the mother hen, the chicks will tend to move toward the mother hen, the location with the most food. Depending on the distance from the chicks to the position of the mother hen, the movement speed of the chicks will be different. With chicks near the mother hen, the new position of the chick is updated using (9)

$$\left[\begin{array}{l} d_{r,j}(k+1)=d_{r,j}(k)+\partial_{up}/k;\text{if } d_{r,best}(k)-\partial_{up}<d_{r,j}(k)<d_{r,best}(k),\\ d_{r,j}(k+1)=d_{r,j}(k)-\partial_{up}/k;\text{if } d_{r,best}(k)+\partial_{up}>d_{r,j}(k)>d_{r,best}(k).\end{array}\right] \quad (9)$$

Otherwise, using (10) for the chicks away from the mother hen

$$\left[\begin{array}{l} d_{r,j}(k+1)=d_{r,j}(k)+\partial_{up};\text{if } d_{r,j}(k)<d_{r,best}(k)-\partial_{up},\\ d_{r,j}(k+1)=d_{r,j}(k)-\partial_{up};\text{if } d_{r,j}(k)>d_{r,best}(k)+\partial_{up},\end{array}\right] \quad (10)$$

where k is the number of the iterations, $j=1,2,...,N$, with N is the total number of chicks.

Each step of the chicks movement will be updated with its fitness value. The mother hen is responsible for observing and updating this best value. If this new fitness value is greater than the current value of the mother hen, the mother hen will transfer to the newly updated position. The mother hen is also updated according to (11)

$$d_{r,j}(k+1)=d_{r,j}(k)+\partial_{up}/(2k);\text{if } d_{r,j}(k)=d_{r,best}(k). \quad (11)$$

The approach of this proposed solution significantly reduces the amplitude of power fluctuations after each loop compared to the implementation mentioned in [19]. The

process of updating this new position of the chicken swarm is shown in Fig. 4(b) and Fig. 5(b).

The movement of the chicken swarm will end when they satisfy the constraint condition of (12)

$$\left|d_{r,best}(k+1)-d_{r,j}(k+1)\right| \le \partial_{up}. \quad (12)$$

This means that the global region has been found. After completing the global region search process, the proposed hybrid method will switch to the various step size InC algorithm to find the MPP. The flow chart of the hybrid method is seen in Fig. 6.

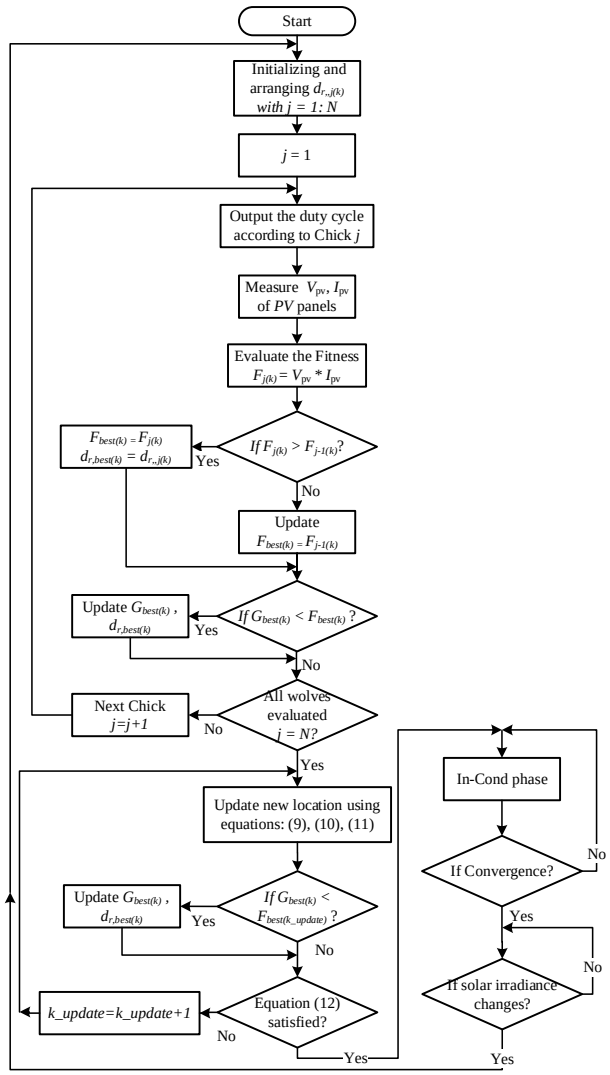

Fig. 6. Flow chart of the proposed hybrid method.

B. *Various Step Size Incremental Conductance (InC) Algorithm*

The incremental conductance (InC) algorithm is usually used to track MPP under uniform solar irradiance conditions. This method is efficient in tracking one peak function. The $\partial P_{pv} / \partial V_{pv}$ slope is used to determine the direction of voltage regulation [21]. This means that it can create $\partial I_{pv} / \partial V_{pv} = 0$ in response to changes in atmospheric circumstances (temperature, solar irradiance), increasing the logical judgment of the output power compared to the output voltage while maintaining the MPP. However, the InC algorithm has a major drawback, which is the large oscillation amplitude around the MPP.

From (12), the best global duty ratio d_{Gbest} is obtained. The proposed various step size InC algorithm is implemented at this duty ratio position. Since the proposed InC algorithm starts at a position close to the true value, the various step sizes only need a few steps to reach the global MPP value. The step size value will gradually decrease after each step. With an initial value of the duty ratio is ∂d_r, after 10 steps, the obtained value is about $0.0135\partial d_r$. The equation of the step size change is shown below

$$V = 1.5385e^{-0.431S}. \quad (13)$$

where S is the number of steps, V is the various step size value; this value is set based on the data mentioned above and used the tool in Microsoft Excel to build the function as seen in Fig. 7. With this implementation, the oscillation amplitude will be significantly reduced and considered to be zero after a few steps of implementing the proposed various step size InC algorithm. The flow chart of the proposed various step size InC algorithm is exhibited as shown in Fig. 8.

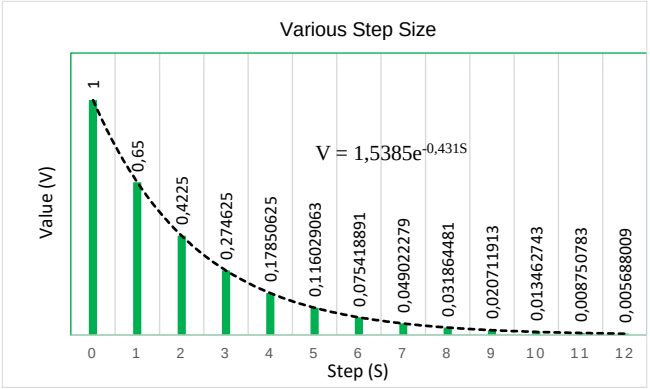

Fig. 7. Various step sizes for the InC algorithm.

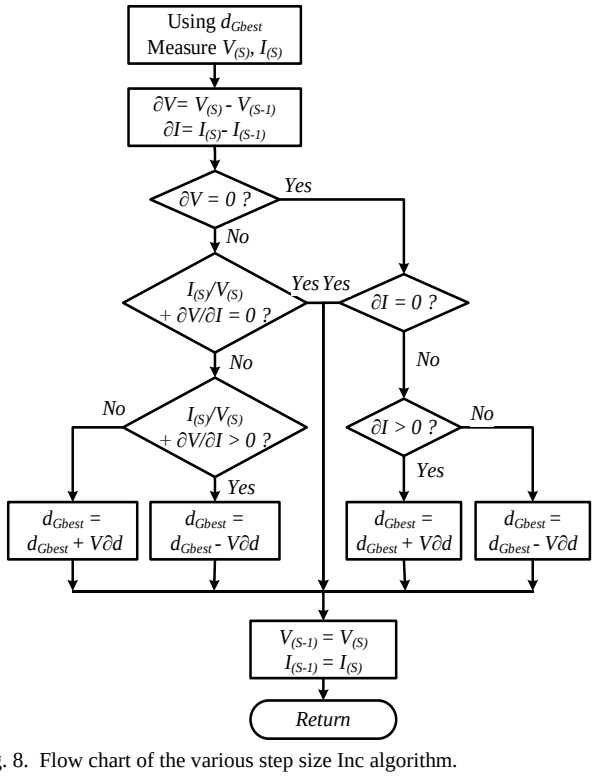

Fig. 8. Flow chart of the various step size Inc algorithm.

Remark: The proposed improved CSO method is used to search for the global maximum power region, so the large step can be used to quickly identify the global region. Taking advantage of the merits of the proposed various step size InC algorithm, the proposed hybrid method has achieved accurate MPP with almost zero fluctuation amplitude and reduced search time. On the other hand, the new position update of the improved CSO method tends to move to a better position than the traditional methods. Finally, MPP was found with high accuracy and no oscillation around MPP. Therefore, the convergence time of the hybrid method is less than that of other methods, such as improved PSO [22], ant colony optimisation (ACO) [23], enhanced grey wolf optimization (GWO) [24], bat algorithm (BA) [25], and other hybrid methods [26], [27].

IV. Simulation Results

MATLAB software is used to simulate the different algorithms. The specifications of the PV panel are shown in Table II. The PV panel system is connected as shown in Fig. 3. For the metaheuristic algorithm used in these simulations, the number of particles is 8. The improved CSO switched to the proposed InC algorithm after satisfying the condition of (13). Each graph displays the simulation results; we divided them into two cases, each case is simulated in 4.0 seconds.

Each duty ratio has an operating time of 10,000 milliseconds or 200 sampling cycles. The components of the boost converter are as follows: C_{in} = 330e-6 F for the input capacitor, L = 300e-5 H for the inductor, C_{out} = 470e-6 F for the output capacitor, R_{load} = 44 Ω for the resistance load, and 20 kHz for the control frequency of the boost converter. The standard GWO, PSO methods are chosen to consider and analyse the efficiency in terms of the global MPP searching, as well as their convergence time to validate the benefits of the suggested hybrid.

TABLE II. THE SPECIFICATIONS OF THE PV PANEL 200 *W*.

Description	Value
Maximum operating voltage (V_{max})	26.3 V
Maximum operating current (I_{max})	7.61 A
Maximum output power (P_{max})	200 W ±10 %
PV cell in parallel (N_p)	1 pcs
PV cell in series (N_s)	54 pcs
Open circuit voltage (V_{oc})	32.9 V
Short circuit current (I_{sc})	8.21 A
P-N junction parameter (B_s)	1.8

A. *Optimisation Simulations for the Cases of One Peak and Two Peaks (Case 1)*

Under uniform solar irradiance, the PV panels receive the same intensity (80 mW/cm^2). A peak is created on the P-V curve as shown in Fig. 9 (the magenta line). The PV system is used with two connected panels in series. The result of this MPP search is shown in Figs. 10, 11, and 12, (situation 1: from 0 to 4.0 seconds). All three GWO, PSO, and proposed hybrid methods achieve the global MPP. However, the GWO and PSO methods take the most time to reach the global MPP. Under partial shading effects, the solar irradiance intensities are set as seen in Fig. 9 with 80 mW/cm^2 and 56 mW/cm^2 for the panel 1 and 2, respectively (the black line). The results of this MPP tracking are displayed in Figs. 10, 11, and 12 (situation 2: from 4.0 to 8.0 seconds).

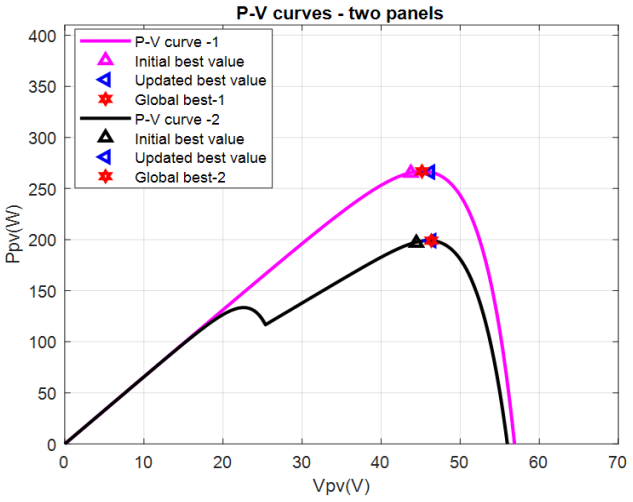

Fig. 9. P-V characteristics of two serial PV panels of the proposed hybrid method.

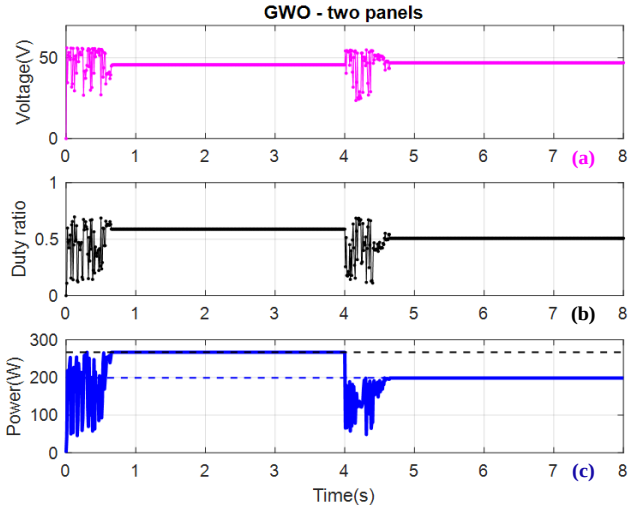

Fig. 10. Trajectories of the GWO method for two serial PV panels in a partially shaded environment: (a) Voltage; (b) Duty ratio; (c) Power.

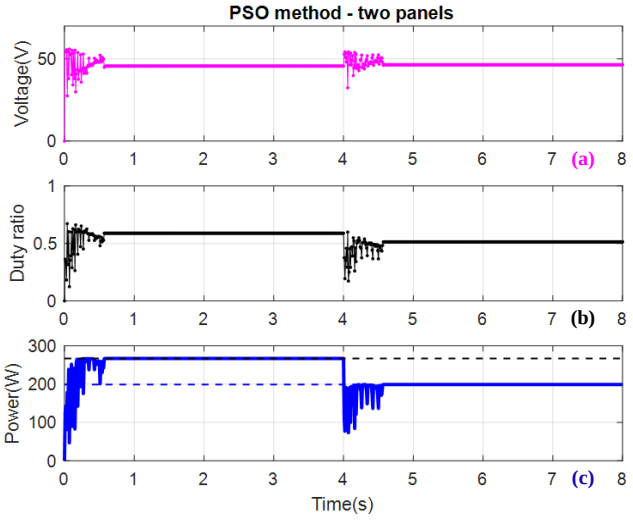

Fig. 11. Trajectories of the PSO method for two serial PV panels in a partially shaded environment: (a) Voltage; (b) Duty ratio; (c) Power.

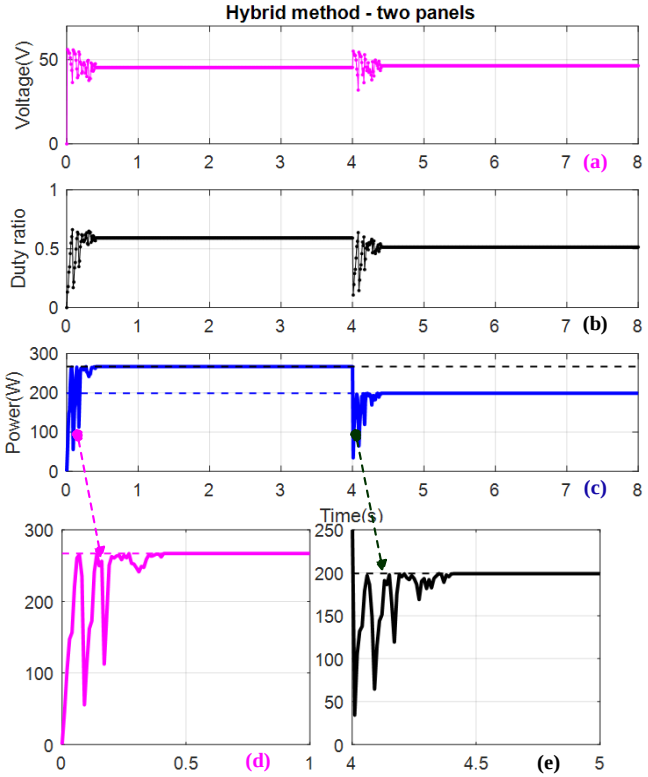

Fig. 12. Trajectories of the proposed method for two serial PV panels in a partially shaded environment: (a) Voltage; (b) Duty ratio; (c) Power; (d) The exaggerated results of power for situation 1; (e) The exaggerated results of power for situation 2.

In these situations, all above mentioned methods also obtain the global MPP, nevertheless, the proposed method is used less time than the GWO and PSO methods.

B. Optimisation Simulations for the Case of Four Peaks (Case 2)

In this case, the two scenarios are set up to produce approximately the same power peaks. This creates a challenge for solutions to find global MPPs because they easily fall into the local traps. The efficiency of the proposed method is seen in all situations as shown in Fig. 13. Each situation has four peaks due to the partial shading conditions that affect the four PV panels with different intensities (Fig. 14). As in the case mentioned above, all methods also achieve the global MPP in all two circumstances. With reasonable organisation and arrangement, the proposed hybrid method not only tends to move toward the global MPP but also converges faster than the GWO and PSO methods.

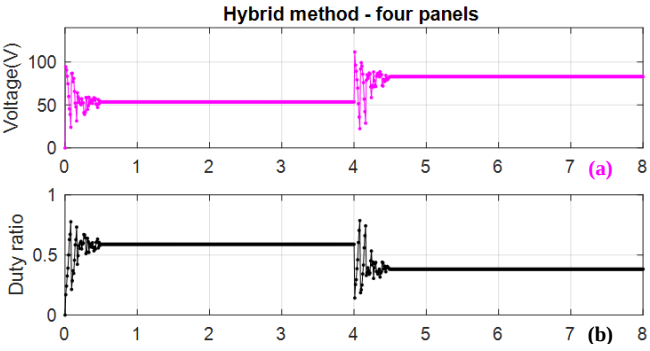

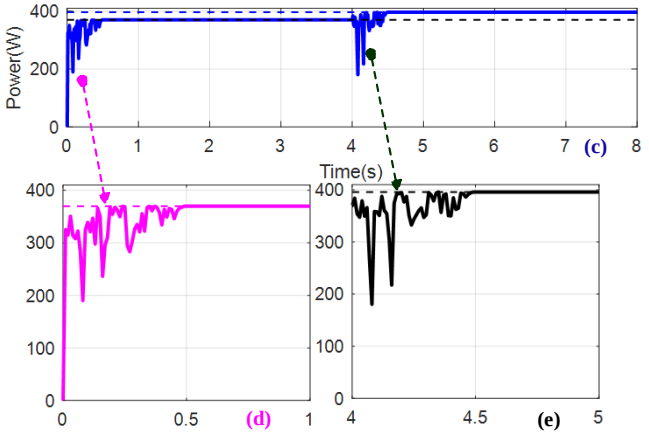

Fig. 13. Trajectories of the proposed method for four serial PV panels in a partially shaded environment: (a) Voltage; (b) Duty ratio; (c) Power; (d) The exaggerated results of power for situation 1; (e) The exaggerated results of power for situation 2.

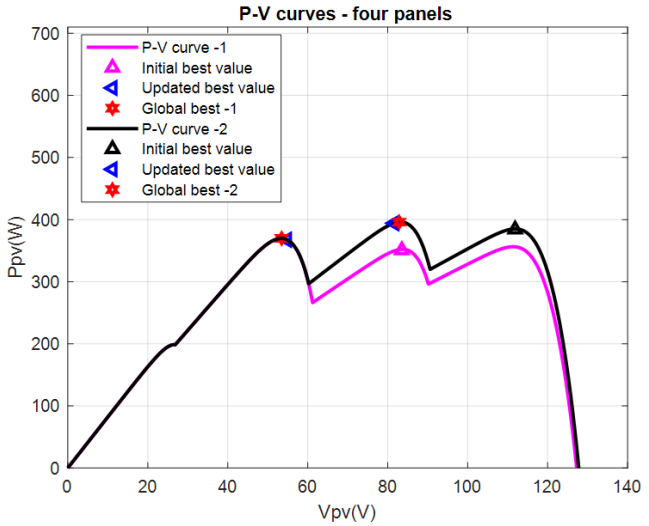

Fig. 14. P-V characteristics of four serial PV panels for partial shading scenarios.

The efficiency of the proposed method is also expressed by comparing with the initial random duty ratio case of the GWO, PSO methods, corresponding to Fig. 13 versus Figs. 15 and 16.

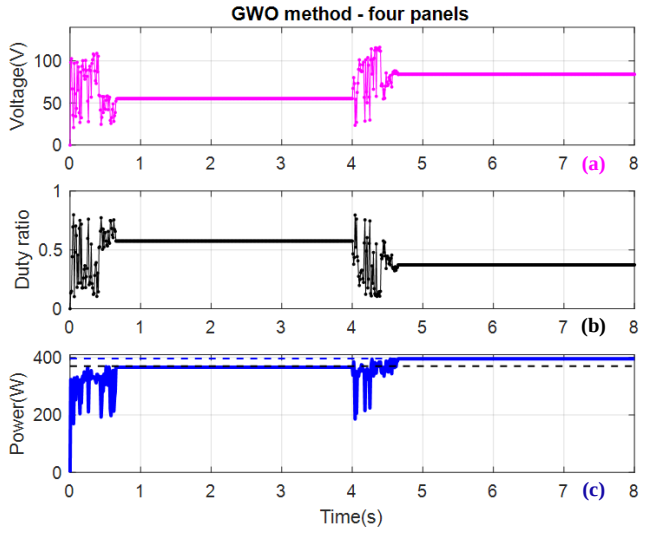

Fig. 15. Trajectories of the GWO method for four serial PV panels in a partially shaded environment: (a) Voltage; (b) Duty ratio; (c) Power.

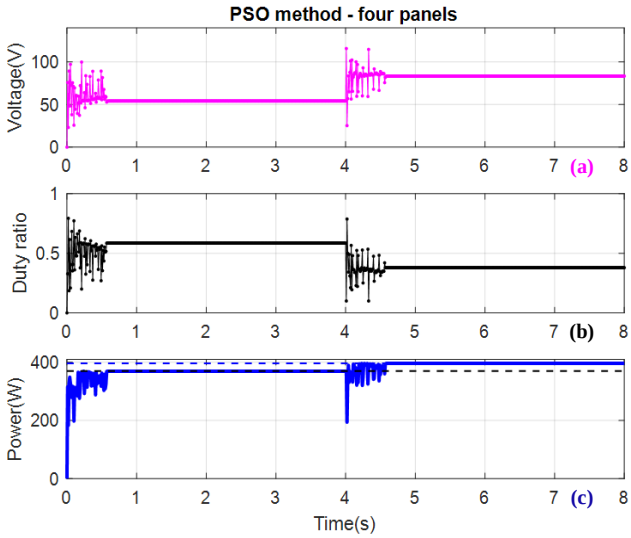

Fig. 16. Trajectories of the PSO method for four serial PV panels in a partially shaded environment: (a) Voltage; (b) Duty ratio; (c) Power.

This result once again indicates the advantages of the recommended hybrid method (HM) with faster convergence to global MPP and shorter duration of oscillations in the PV output power (see Table III).

TABLE III. MPP TRACKING RESULTS WITH DIFFERENT SITUATIONS.

Case	Irradiance intensity (mW/cm^2)	Ideal power at global MPP (W)	GWO	PSO	HM
			Time (s)	Time (s)	Time (s)
1 (2 panels)	[80, 80]	267.0	0.66	0.57	0.41
	[80, 56]	199.1	0.66	0.57	0.41
2 (4 panels)	[100 ,90, 53, 40]	369.6	0.67	0.59	0.49
	[100, 90, 60, 43]	396.0	0.67	0.58	0.49

V. EXPERIMENTAL RESULTS

A. Circuit Design for MPP Tracking Strategy of Stand-Alone PV Energy Systems

Table II provides information on the characteristics of the PV power panel used to carry out the experiment. In this experiment, two panels are wired in series and exposed to radiation of 80–80 mW/cm^2 in scenario 1 and 80–56 mW/cm^2 in the other, respectively. The global MPPs of these two situations are 267 W for situation 1 and 199.1 W for situation 2 as seen in Figs. 9–12. A bypass diode (Fig. 1) is used to link each panel in the shunt in the experimental model, which is based on the setup depicted in Fig. 3. The DC/DC boost converter is controlled by an ARDUINO Mega2560 board to evaluate the proposed hybrid MPP searching method and GWO and PSO methods. The methods execute each duty ratio value for 20 milliseconds to record the PV current and voltage values of the power system through the voltage divider and current sensor. The basic parameters of the boost converter are the inductor L = 1.4 mH, the input capacitor C = 470 μF /200 V, the output capacitor C = 330 μF /450 V, the MOSFET Q = $IRFP250N$, the fast switching diode D = $MBR30200PT$, and the resistant load R_{load} = 45 Ω. . The experimental model is shown in Fig. 17.

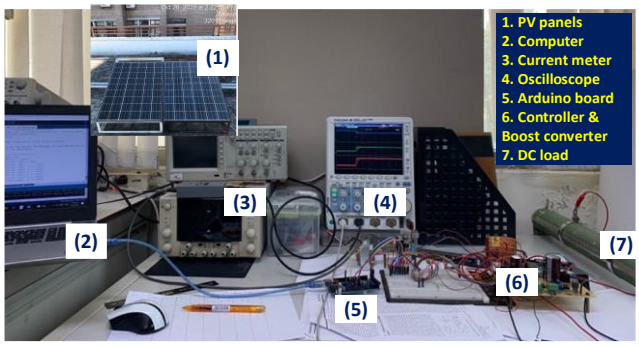

Fig. 17. Practical experimental model for a stand-alone PV system.

B. Experimental Results and Discussion

Under uniform weather conditions, the measured solar radiance intensity on the two PV panels has the same value of 80 mW/cm^2. And under the partial shading effect, the measured solar radiance intensity on the two PV panels has different values of 80 mW/cm^2 and 56 mW/cm^2. The simulation results are represented as shown in Figs. 9–12. With the GWO method, the experimental results are displayed in Fig. 18 with 6.5 A, 40 V, 267 W (from top to bottom) for situation 1, and 4.91 A, 40.5 V, 199 W for situation 2. This GWO method takes 1.5 and 1.3 seconds to obtain the global MPPs. The experimental results of the PSO and proposed methods are displayed in detail, as shown in Figs. 19 and 20. The PSO and proposed hybrid methods also achieve the same values as the GWO, but they quickly achieve the global MPPs. The PSO obtains the global MPPs with 0.8 and 0.9 seconds for scenarios 1 and 2, sequentially. The experimental results are shown in Fig. 20 for the proposed hybrid method with a time to reach the global MPP of 0.5 seconds for both scenarios 1 and 2, respectively. From the results shown in Figs. 18–20, it shows that the proposed method not only has the fastest time to reach the global MPP, but also has the low amplitude of the oscillation. The amplitude of the oscillation is reduced because the power values in the subsequent loops tend to gradually move towards the global MPP. These are the outstanding advantages of the proposed method compared with the PSO and GWO methods.

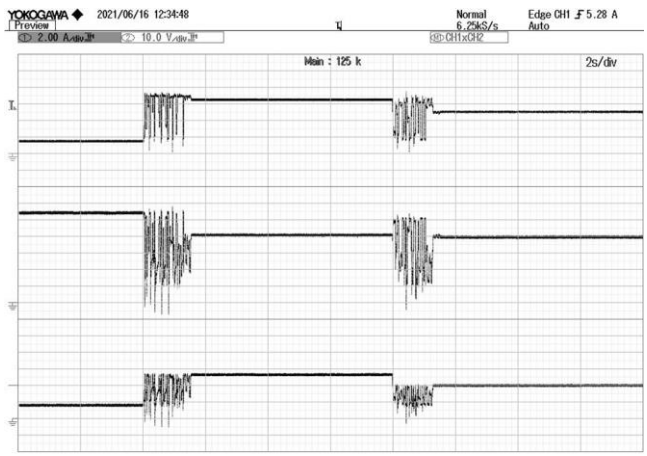

Fig. 18. Experimental trajectories for two serial PV panels using the GWO method (from top to bottom: current, voltage, power).

The findings have shown that the suggested hybrid technique can track the global MPP under partial shading effects, as well as under conditions of uniform solar

irradiance intensity. Although the global MPP can be searched using the GWO, PSO approaches, and other MPP methods, the novel hybrid method exhibits reduced voltage and power oscillation.

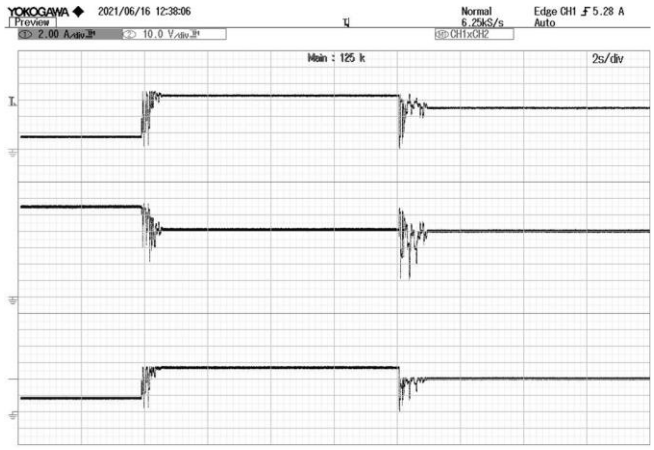

Fig. 19. Experimental trajectories for two serial PV panels using the PSO method (from top to bottom: current, voltage, power).

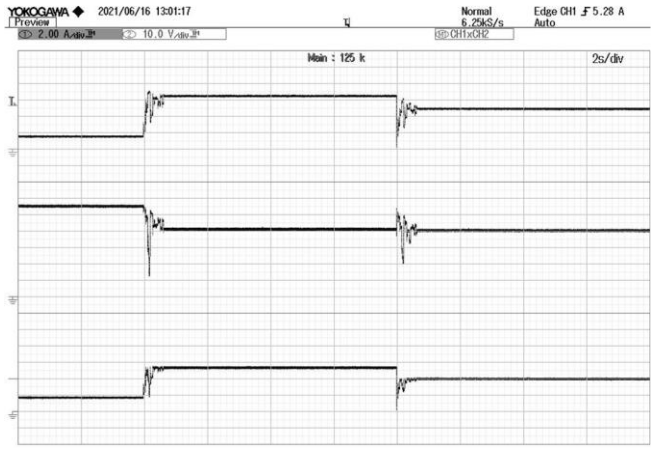

Fig. 20. Experimental trajectories for two serial PV panels using the proposed method (from top to bottom: current, voltage, power).

On the basis of fast convergence, the efficiency and high accuracy of the proposed hybrid method are also demonstrated. In addition, as the number of initial members of the chick increases, the accuracy of the proposed technique increases. Therefore, a high-speed microcontroller must be replaced in order to react quickly to changes in actual weather conditions.

VI. CONCLUSIONS

By organising and updating duty ratio values according to the new approach, the proposed method is not only simple in the calculation, but also faster in convergence than the PSO and GWO methods, as shown in Table III and the experimental results. Furthermore, the use of a boost converter for the MPP tracking design with initial location arrangement and area division of the duty ratio prevented the improved CSO method from falling into local traps. The simulation and experimental results presented above have demonstrated that this control strategy has been successful in searching the global region, and the InC algorithm will help to reach the maximum power point in this global region. Therefore, the proposed hybrid method has achieved the expected results. It achieves the best power conversion efficiency. In addition, the ability to fast convergence and decreasing amplitude of oscillation are also the highlights of this proposed hybrid method.

CONFLICTS OF INTEREST

The authors declare that they have no conflicts of interest.

REFERENCES

[1] W. Zhu, L. Shang, P. Li, and H. Guo, “Modified hill climbing MPPT algorithm with reduced steady-state oscillation and improved tracking efficiency”, *The Journal of Engineering*, vol. 2018, no. 17, pp. 1878–1883, 2018. DOI: 10.1049/joe.2018.8337.

[2] J. Ahmed, Z. Salam, M. Kermadi, H. N. Afrouzi, and R. H. Ashique, “A skipping adaptive P&O MPPT for fast and efficient tracking under partial shading in PV arrays”, *International Transactions on Electrical Energy Systems*, vol. 31, no. 9, p. e13017, 2021. DOI: 10.1002/2050-7038.13017.

[3] R. Ahmad, A. F. Murtaza, and H. A. Sher, “Power tracking techniques for efficient operation of photovoltaic array in solar applications – A review”, *Renewable and Sustainable Energy Reviews*, vol. 101, pp. 8–102, 2019. DOI: 10.1016/j.rser.2018.10.015.

[4] A. N. Mahmod Mohammad, M. A. Mohd Radzi, N. Azis, S. Shafie, and M. A. Atiqi Mohd Zainuri, “An enhanced adaptive perturb and observe technique for efficient maximum power point tracking under partial shading conditions”, *Applied Sciences*, vol. 10, no. 11, p. 3912, 2020. DOI: 10.3390/app10113912.

[5] H. F. Hashim, M. M. Kareem, W. K. Al-Azzawi, and A. H. Ali, “Improving the performance of photovoltaic module during partial shading using ANN”, *International Journal of Power Electronics and Drive Systems (IJPEDS)*, vol. 12, no. 4, pp. 2435–2442, 2021. DOI: 10.11591/ijpeds.v12.i4.pp2435-2442.

[6] A. M. Eltamaly, H. M. H. Farh, and A. G. Abokhalil, “A novel PSO strategy for improving dynamic change partial shading photovoltaic maximum power point tracker”, *Energy Sources, Part A: Recovery, Utilization, and Environmental Effects*, pp. 1–15, 2020. DOI: 10.1080/15567036.2020.1769774.

[7] T. Nagadurga, P. V. R. L. Narasimham, V. S. Vakula, and R. Devarapalli, “Gray wolf optimization-based optimal grid connected solar photovoltaic system with enhanced power quality features”, *Concurrency and Computation: Practice and Experience*, vol. 34, 2021. DOI: 10.1002/cpe.6696.

[8] I. Shams, S. Mekhilef, and K. S. Tey, “Maximum power point tracking using modified butterfly optimization algorithm for partial shading, uniform shading, and fast varying load conditions”, *IEEE Transactions on Power Electronics*, vol. 36, no. 5, pp. 5569–5581, 2021. DOI: 10.1109/TPEL.2020.3029607.

[9] N. Hashim and Z. Salam, “Critical evaluation of soft computing methods for maximum power point tracking algorithms of photovoltaic systems”, *International Journal of Power Electronics and Drive Systems (IJPEDS)*, vol. 10, no. 1, pp. 548–561, 2019. DOI: 10.11591/ijpeds.v10.i1.pp548-561.

[10] B. Yang *et al.*, “PV arrays reconfiguration for partial shading mitigation: Recent advances, challenges and perspectives”, *Energy Conversion and Management*, vol. 247, art. 114738, 2021. DOI: 10.1016/j.enconman.2021.114738.

[11] M. H. Zafar *et al.*, “A novel meta-heuristic optimization algorithm based MPPT control technique for PV systems under complex partial shading condition”, *Sustainable Energy Technologies and Assessments*, vol. 47, art. 101367, 2021. DOI: 10.1016/j.seta.2021.101367.

[12] A. M. Eltamaly, “An improved cuckoo search algorithm for maximum power point tracking of photovoltaic systems under partial shading conditions”, *Energies*, vol. 14, no. 4, p. 953, 2021. DOI: 10.3390/en14040953.

[13] D. Pilakkat and S. Kanthalakshmi, “An improved P&O algorithm integrated with artificial bee colony for photovoltaic systems under partial shading conditions”, *Solar Energy*, vol. 178, pp. 37–47, 2019. DOI: 10.1016/j.solener.2018.12.008.

[14] G. S. Chawda, O. P. Mahela, N. Gupta, M. Khosravy, and T. Senjyu, “Incremental conductance based particle swarm optimization algorithm for global maximum power tracking of solar-PV under nonuniform operating conditions”, *Applied Sciences*, vol. 10, no. 13, p. 4575, 2020. DOI: 10.3390/app10134575.

[15] J. Ding, Q. Wang, Q. Zhang, Q. Ye, and Y. Ma, “A hybrid particle swarm optimization-Cuckoo Search algorithm and its engineering

applications", *Mathematical Problems in Engineering*, vol. 2019, art. ID 5213759, 2019. DOI: 10.1155/2019/5213759.

[16] S. Ngo, C.-S. Chiu, and P.-T. Nguyen, "MPPT design using the hybrid method for the PV system under partial shading conditions", in *Research in Intelligent and Computing in Engineering. Advances in Intelligent Systems and Computing*, vol. 1254. Springer, Singapore, 2021, pp. 77–87. DOI: 10.1007/978-981-15-7527-3_8.

[17] E. Irmak and N. Güler, "A model predictive control-based hybrid MPPT method for boost converters", *International Journal of Electronics*, vol. 107, no. 1, pp. 1–16, 2020. DOI: 10.1080/00207217.2019.1582715.

[18] C.-S. Chiu and S. Ngo, "Hybrid SFLA MPPT design for multi-module partial shading photovoltaic energy systems", *International Journal of Electronics*, vol. 110, no. 1, pp. 199–220, 2023. DOI: 10.1080/00207217.2021.2025443.

[19] C.-S. Chiu and S. Ngo, "A novel algorithm-based MPPT strategy for PV power systems under partial shading conditions", *Elektronika ir Elektrotechnika*, vol. 28, no. 1, pp. 42–51, 2022. DOI: 10.5755/j02.eie.30183.

[20] X. Meng, Y. Liu, X. Gao, and H. Zhang, "A new bio-inspired algorithm: Chicken Swarm Optimization", in *Advances in Swarm Intelligence. ICSI 2014. Lecture Notes in Computer Science*, vol. 8794. Springer, Cham, 2014, pp. 86–94. DOI: 10.1007/978-3-319-11857-4_10.

[21] S. Ngo and C. S. Chiu, "Simulation implementation of MPPT design under partial shading effect of PV panels", in *Proc. of 2020 International Conference on System Science and Engineering (ICSSE)*, 2020, pp. 1–6. DOI: 10.1109/ICSSE50014.2020.9219306.

[22] A.-w. Ibrahim *et al.*, "PV maximum power-point tracking using modified particle swarm optimization under partial shading conditions", *Chinese Journal of Electrical Engineering*, vol. 6, no. 4, pp. 106–121, 2020. DOI: 10.23919/CJEE.2020.000035.

[23] S. Krishnan G., S. Kinattingal, S. P. Simon, and P. S. R. Nayak, "MPPT in PV systems using ant colony optimisation with dwindling population", *IET Renewable Power Generation*, vol. 14, no. 7, pp. 1105–1112, 2020. DOI: 10.1049/iet-rpg.2019.0875.

[24] R. Motamarri, N. Bhookya, and B. C. Babu, "Modified grey wolf optimization for global maximum power point tracking under partial shading conditions in photovoltaic system", *International Journal of Circuit Theory and Applications*, vol. 49, no. 7, pp. 1884–1901, 2021. DOI: 10.1002/cta.3018.

[25] C. Y. Liao, R. K. Subroto, I. S. Millah, K. L. Lian, and W.-T. Huang, "An improved bat algorithm for more efficient and faster maximum power point tracking for a photovoltaic system under partial shading conditions", *IEEE Access*, vol. 8, pp. 96378–96390, 2020. DOI: 10.1109/ACCESS.2020.2993361.

[26] A. M. Eltamaly and H. M. H. Farh, "Dynamic global maximum power point tracking of the PV systems under variant partial shading using hybrid GWO-FLC", *Solar Energy*, vol. 177, pp. 306–316, 2019. DOI: 10.1016/j.solener.2018.11.028.

[27] N. Priyadarshi, S. Padmanaban, J. B. Holm-Nielsen, F. Blaabjerg, and M. S. Bhaskar, "An experimental estimation of hybrid ANFIS–PSO-based MPPT for PV grid integration under fluctuating sun irradiance", *IEEE Systems Journal*, vol. 14, no. 1, pp. 1218–1229, 2020. DOI: 10.1109/JSYST.2019.2949083.